OUTSTANDING NATURAL OCCURRENCE OF TiO_2–II AT THE CHICXULUB CRATER – ANATOMY OF A SHOCK-PRODUCED HIGH-PRESSURE POLYMORPH

Martin Schmieder[1,2], Timmons M. Erickson[3,4], Zia Rahman[3,4], Lindsay P. Keller[3], David A. Kring[1,2], and the IODP–ICDP Expedition 364 Science Party,
[1]Lunar and Planetary Institute – USRA, Houston, TX 77058 USA (martin@suevite.com), [2]NASA – SSERVI, [3]NASA Johnson Space Center, Houston, TX 77058 USA, [4]Jacobs JETS, NASA/JSC, Houston, TX 77058 USA.

Introduction and Background: Scientific drilling of the end-Cretaceous, ~180 km-diameter Chicxulub crater (Yucatán Peninsula, Mexico) during IODP–ICDP Expedition 364 has provided new insights into the formation, shock metamorphism, structural evolution, and thermal history of peak rings in large complex impact craters [1–6]. An outstanding feature in uplifted granitoid rocks of the Chicxulub peak ring is the preservation of TiO_2–II, an orthorhombic high-pressure polymorph of TiO_2 with an α-PbO_2 structure [7,8], produced during the impact from rutile and/or anatase at shock pressures of ~12.5–17.5 GPa [4]. Unlike other mostly micro- and cryptocrystalline occurrences of TiO_2–II at terrestrial impact sites, ejecta deposits ([9,10] and references therein), and in rare ultra-high pressure metamorphic rocks [11], TiO_2–II at Chicxulub occurs as abundant euhedral crystals ≤70 µm in size within aggregates of altered magmatic titanite. This mode of occurrence provides an excellent opportunity to investigate the crystallography and transformation kinetics of the shock-produced high-pressure polymorph using scanning electron microscopic, micro-Raman, electron backscatter diffraction (EBSD) [9,10], focused ion beam (FIB), as well as transmission-EBSD and transmission electron microscopic (TEM) techniques. Here we present refined microstructural and new crystallographic results for TiO_2–II at the Chicxulub crater.

Sample and Analysis: TiO_2 in shocked granitoid rock sample 174–2–19–20 (core depth 949 m below seafloor [1,2,9,10]) from the Chicxulub peak ring was analyzed using a 7600f JEOL field emission gun scanning electron microscope (FEG-SEM) with an Oxford Instruments Symmetry EBSD detector for phase and orientation mapping and transmission-EBSD; a Quanta 3D FEG for FIB sectioning; and a JEOL 2500 field-emission scanning-transmission electron microscope (FE-STEM) for diffraction pattern analysis, indexing, and the determination of unit cell parameters at the NASA Johnson Space Center.

Results and Interpretation: High-resolution EBSD mapping of TiO_2 crystals (Fig. 1A) reveals a complex arrangement of lamellar and granular crystal domains. TiO_2–II, which commonly forms larger, coherent, lamellar subdomains (Fig. 1B), is the dominant mineral phase. Rutile occurs as microcrystalline granules and lamellae that locally overprint shock-produced TiO_2–II and is, thus, interpreted as a post-shock reversion product. Individual TiO_2–II lamellae are related to one another by rational twin orientations (Fig. 1C), indicating twinning occurred during the solid-state transformation to minimize intracrystalline strain energy. Three dominant twin orientations are observed with a disorientation axis of 87°/<010>, 55°/<010>, and 85°/<100>. Moreover, TiO_2–II and neoblastic rutile are systematically misoriented from one another, suggesting the solid-state TiO_2–II-to-rutile reversion is crystallographically controlled. High-resolution transmission-EBSD and TEM analyses were carried out to further characterize the nanostructure and unit cell parameters in natural, shock-produced TiO_2–II. Results from TEM electron diffraction analysis and indexing are consistent with the unit cell parameters of experimentally produced TiO_2–II [12]. These results underline the outstanding natural occurrence of TiO_2–II at the Chicxulub impact crater, which may be an appropriate type locality for this high-pressure polymorph.

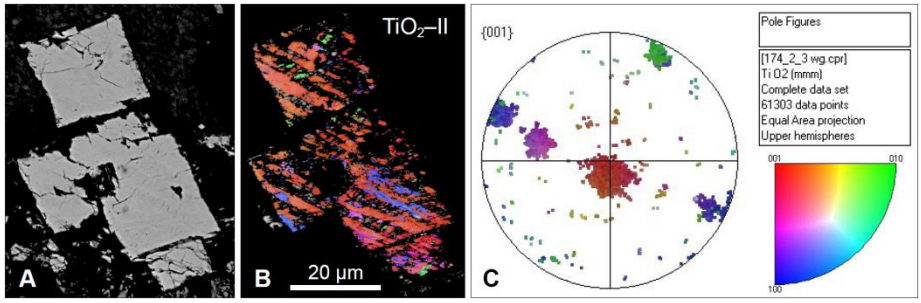

Fig. 1: TiO_2–II in shocked granitoid rock from the Chicxulub peak ring (sample 174–2–19–20). **A:** Back-scattered electron image of TiO_2 crystals. **B:** EBSD inverted pole figure map of TiO_2–II. **C:** Pole figure corresponding to map shown in B (IPF-z).

References: [1] Morgan J. V. et al. (2016) *Science*, 354, 878–882. [2] Gulick S. P. S. et al. (2017) Exp. 364 Prelim. Rep., IODP, 38 pp. [3] Kring D. A. et al. (2017) *GSA Today*, 27, 5 pp. [4] Rae A. S. P. et al. (2017) *LPS XLVIII*, abstr. #1934. [5] Kring D. A. et al. (2017) *LPS XLVIII*, abstr. #1212. [6] Kring D. A. et al. (2016) *Nature Comm.*, 7, 13161. [7] Linde R. K. and DeCarli P. S. (1969) *J. Chem. Phys.*, 50, 319–325. [8] El Goresy A. et al. (2001) *EPSL*, 192, 485–495. [9] Schmieder M. et al. (2017) 80th MetSoc, abstr. #6134. [10] Schmieder M. et al. (2019) *LPS XLIX*, abstr. #1658. [11] Shen P. et al. (2001) *Int. Geol. Rev.*, 43, 366–378. [12] Gerward, L. and Staun Olsen, J. (1997) *J. Appl. Cryst.*, 30, 259–264.